Vertical Transport in Semiconductor Superlattices Probed by Miniband-to-Acceptor Magnetoluminescence

B. J. Skromme
Department of Electrical Engineering, Arizona State University, Tempe, Arizona 85287-5706

R. Bhat, M. A. Koza, S. A. Schwarz, T. S. Ravi, and D. M. Hwang
Bellcore, Redbank, New Jersey 07701
(Received 24 July 1990)

The cyclotron motion of electrons in coupled-well AlGaAs/GaAs superlattices is investigated by photoluminescence of conduction-band to acceptor transitions in magnetic fields up to 13 T, applied either parallel or perpendicular to the layers. For parallel fields, three different regimes are observed as the ratio of the cyclotron radius to the superlattice period is reduced, namely, tunneling cyclotron motion within the miniband, miniband breakdown, and finally a transition from electric to magnetic quantization. A fully quantum-mechanical calculation agrees well with experiment.

PACS numbers: 73.20.Dx, 73.40.Kp, 78.55.Cr, 78.65.Fa

Semiconductor superlattices, by virtue of their widely tunable properties, offer the unique opportunity to explore physical phenomena that are typically not accessible in naturally occurring solids. Notable examples are the possibility of achieving Bloch oscillation or related negative differential conductivity effects,[1] the observation of Wannier-Stark ladders under strong applied electric fields,[2] and the behavior of cyclotron orbits in a layered structure when the magnetic length becomes comparable to the layer period.[3] Here we focus on the last of these phenomena, i.e., the physics of cyclotron motion in the presence of a periodic one-dimensional superlattice potential, whose period may be made smaller than, larger than, or comparable to the orbit diameter. The study of this cyclotron motion provides critical insight into the miniband structure and related vertical transport phenomena in the superlattice.

Previous investigations of cyclotron motion in superlattices have employed either photoluminescence (PL) excitation spectroscopy of exciton states[3,4] or far-infrared cyclotron resonance involving only electrons in the minibands.[5-7] In both experiments, the Landau levels were found to be essentially unperturbed from bulk-GaAs-like behavior for fields perpendicular to the layers.[3-7] For parallel fields, however, a heavier cyclotron mass is observed for Landau levels remaining within the original miniband, while at higher energies the levels become dispersive and strongly dependent on the position of the orbit center with respect to the wells and barriers.[3-7] This behavior is in agreement with numerical solutions of Schrödinger's equation, as originally discussed by Maan.[4]

While these experiments yielded considerable insight into the relationship between cyclotron motion and miniband structure, the experimental techniques themselves complicate the quantitative interpretation of the results. In excitation spectroscopy, the holes involved in the exciton states contribute to the observed diamagnetism in ways that are extremely complex, due to the degenerate, anisotropic nature of the valence band. Moreover, the excitonic binding also affects the observed diamagnetism (especially for the lowest level), and spin splittings of the electron and hole should be considered in the analysis. Cyclotron resonance is affected by interactions with plasmon modes, which are highly complex in superlattices.[5,7] Also, complicated experimental techniques such as employing ratios of spectra or electric-field modulation (which might affect the miniband transport[2]) are necessary[5-7] and only the *joint* density of states between Landau levels can be probed.

In the following, we propose and demonstrate a novel scheme that circumvents many of the limitations of the other experimental techniques, while providing a highly complementary viewpoint. The technique consists in observing the PL from recombination of electrons in the lowest Landau level(s), where they reside by virtue of thermalization, with holes localized on acceptors near the center of the GaAs wells (denoted e-A^0 transitions). These holes have completely negligible diamagnetism,[8] and their spin splittings are known exactly from studies on bulk GaAs.[8] The experimental behavior of the electron Landau levels can therefore be determined unambiguously from the e-A^0 peak positions. Complications due to the valence band, excitons, and plasmons are avoided, the experiments are easily performed, and we can isolate the behavior of individual Landau levels (although only the lowest is typically observable).

Possible complications in this scheme include the presence of both donor-to-acceptor (D^0-A^0) and e-A^0 peaks in the spectra,[9] and the well-known dispersion in the acceptor binding energy as a function of position along the growth axis.[9,10] These effects are minimized by performing the measurements at moderately elevated temperatures (15–25 K), where the D^0-A^0 peaks are suppressed by thermal ionization of the donors, and differential thermal ionization of the shallower barrier acceptors en-

TABLE I. Target and measured superlattice parameters.

Period (Å)		Well width (Å)		Barrier width (Å)		Ave. Al content		Al content in barriers	
Target	Meas.	Target	Meas.	Target	Meas.	Target	Meas.	Target	Meas.
100	90	80	64	20	26	0.06	0.062	0.3	0.21
200	153	180	135	20	18	0.03	0.029	0.3	0.25
600	550	590	540	10	10	0.005	0.0049	0.3	0.27

sures that we observe only e-A^0 transitions for acceptors in the center of the wells.[9] The pronounced maximum in the acceptor binding-energy density of states for acceptors in this location further ensures a well-defined peak.[9]

The samples were grown by atmospheric-pressure organometallic chemical vapor deposition (OMCVD). They consist of approximately 6-μm-thick GaAs/AlGaAs superlattices, whose target layer thicknesses and compositions are given in Table I. The actual layer thicknesses were determined by transmission electron microscopy (TEM). The average Al content in the samples was determined using a novel secondary-ion mass-spectroscopy (SIMS) technique for composition determination relative to a standard sample using O_2^+ bombardment.[11] The Al compositions of the barriers were estimated from the combination of the TEM and SIMS results, and are shown in Table I. The samples are n type with a carrier concentration of a few $\times 10^{15}$ cm^{-3}, due to residual donor doping (mainly in the barriers).

In Fig. 1 we plot the e-A^0 peak positions for the 90-Å-period superlattice for both parallel and perpendicular fields, together with linear fits to the data points. In both cases the spectra were recorded in σ polarization ($\Delta m_j = \pm 1$), with $\mathbf{B} \| \langle 100 \rangle$; the excitation intensity was about 2.8 mW/cm^2 at 1.581 eV from a dye laser. Temperature-dependent spectra demonstrating the e-A^0 nature of the peaks observed under the present conditions were shown in Ref. 9. The actual magnetic-field-dependent spectra of the D^0-A^0 and e-A^0 peaks are omitted here for brevity, but will be published elsewhere. At low field the peak position increases sublinearly with field, due to the change in the miniband density of states from three dimensional ($\sim E^{1/2}$) to one dimensional ($\sim E^{-1/2}$);[8] the width of this region depends on the temperature. The data points for 3 T and above show a linear dependence on field within the experimental accuracy for *both* field orientations, but with distinctly different slopes. The peak positions E_{peak} in the linear range can be modeled by

$$E_{\text{peak}} = E_g + \Delta E + (n + \tfrac{1}{2})\hbar\omega_c + g_e m_{je}\mu_B B + g_h m_{jh}\mu_B B - E_A ,$$

where E_g is the band gap of bulk GaAs, ΔE is the confinement energy of electrons relative to bulk GaAs at $B=0$, n is the Landau-level index, ω_c is the cyclotron frequency ($=eB/m_c^*$, where m_c^* is the appropriate cyclotron mass), g_e and g_h are the g values of electrons and holes, m_{je} and m_{jh} are the z components of the intrinsic electron and hole angular momenta, μ_B is the Bohr magneton, and E_A is the energy of the acceptor level at the center of the wells *with respect to the valence-band edge of bulk GaAs*. The allowed combinations of m_j values, and corresponding oscillator strengths and g values, are given in Ref. 8.

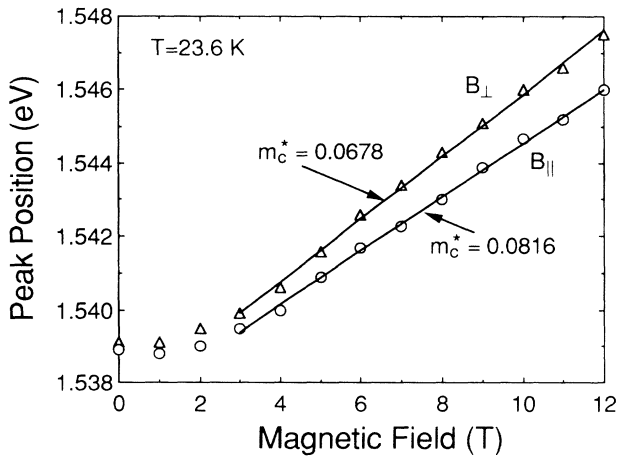

FIG. 1. Positions of the e-A^0 peaks for the 90-Å-period superlattice, for fields parallel (circles) and perpendicular (triangles) to the layers, and linear fits to the data in each case (solid lines).

For these data, we have verified using line-shape calculations that it is a reasonable approximation to ignore the effects of the spin splittings on the slope of the peak position of the total line shape as a function of field. The slopes then give cyclotron masses of 0.0678 and 0.0816 with the field perpendicular and parallel to the layers, respectively. For the perpendicular field the mass is indistinguishable from that observed for bulk GaAs in a similar experiment, 0.0677.[8] This agreement is not surprising, since in this geometry the electrons execute cyclotron motion mainly within the GaAs wells.

For the parallel field, the lowest Landau level remains well within the first miniband, since its width is calculated[12,13] to be 30 meV and the e-A^0 peak shift at 12 T is only 8.5 meV. The cyclotron mass in this geometry is the geometric mean of the superlattice tunneling mass and the in-plane mass.[5] The tunneling mass is thus $(0.0816)^2/0.0678 = 0.098$. We compare this result to the value 0.091 for the bottom of the miniband, determined

from the dispersion relation given by Bastard,[12] neglecting nonparabolicity and using the measured sample parameters in Table I. The small discrepancy is probably due to the neglect of spin splittings. These results demonstrate a clear and direct measurement of the tunneling mass in a superlattice miniband, unencumbered by excitonic or plasmon effects.

A completely different behavior is observed for the 550-Å-period sample, as shown in Fig. 2. Since the temperature favors thermalization into the lowest $(-\frac{3}{2},\frac{1}{2})$ spin component in this case (which is well resolved), we allow for the Zeeman energy of that component in computing the cyclotron masses from the straight-line fits. We obtain 0.066 for the mass in *both* orientations for $B \geq 3$ T. The cyclotron radius varies from 148 Å at 3 T to 74 Å at 12 T, so that orbits near the center of the wells (which dominate the density of states, particularly when thermalization is considered), do not feel the barriers in this range. Thus, the observation of the bulk GaAs mass in both field orientations is entirely reasonable. The peak shift in a 3-T parallel field is already greater than the 0.5-meV width of the lowest miniband, so the miniband picture is of no use in describing the cyclotron motion in this regime. In fact, the shrinking of the cyclotron orbit in the parallel field has led to a transition from "electric" quantization of the energy levels (at $B=0$) to completely "magnetic" quantization ($B \geq 3$ T), in which the barriers no longer affect the wave functions.

The anisotropy in the peak positions as a function of orientation is due to the destruction of the miniband structure and related confinement energy by the parallel field, while the perpendicular field does not affect it. The difference between the e-A^0 peak energies at high field therefore *gives a direct measure of the electron confinement energy at the bottom of the first miniband.* In Fig. 2 this energy is 0.9 meV, in fair agreement with the value 1.4 meV calculated for the bottom of the miniband. The discrepancy may be related to uncertainties in band offsets, sample parameters, etc.

In the intermediate regime, where the cyclotron-orbit diameter is comparable to the superlattice period, neither of the above simple pictures applies. A complicated, nonlinear dependence of peak position on energy is anticipated for parallel fields, and in fact is observed for the 153-Å-period superlattice, as shown in Fig. 3. While the peak shift remains nominally within the lowest miniband (9 meV wide) for most of the field range studied, numerical calculations show that the lowest Landau level develops significant dispersion at several T, which becomes pronounced at 12 T. (This effect may result from the second Landau level exiting the miniband.) We have therefore performed a detailed calculation of the line shape and peak shift as a function of field, which is briefly outlined below.

The PL line shape can be calculated using Fermi's "golden rule" as

$$I_{\mathrm{PL}}(\hbar\omega) \propto \int g(E)f(E)P(E_A)f'(E_A)|\langle e|A^0\rangle|^2\delta(E)dE_A\,,$$

where $I_{\mathrm{PL}}(\hbar\omega)$ is the intensity as a function of photon energy; $E=\hbar\omega-E_g+E_A$ is the energy of an electron with respect to the GaAs conduction-band edge E_g; E_A is a function of the location x_i of the acceptor along the growth axis; $g(E)$ is the electron density of states in the field; $f(E)=e^{-k_BT}$ is the Boltzmann occupation factor for the electron states; $P(E_A)$ is the acceptor-level energy density of states determined from $E_A(x_i)$, assuming a uniform distribution along the growth axis; $f'(E_A)$ is the probability of an acceptor level E_A being occupied by a hole, which we take proportional to $(1+Ce^{-E_A/k_BT})^{-1}$, to allow for thermal depopulation of the shallower acceptor levels (C is an adjustable parameter); $\langle e|A^0\rangle$ is the

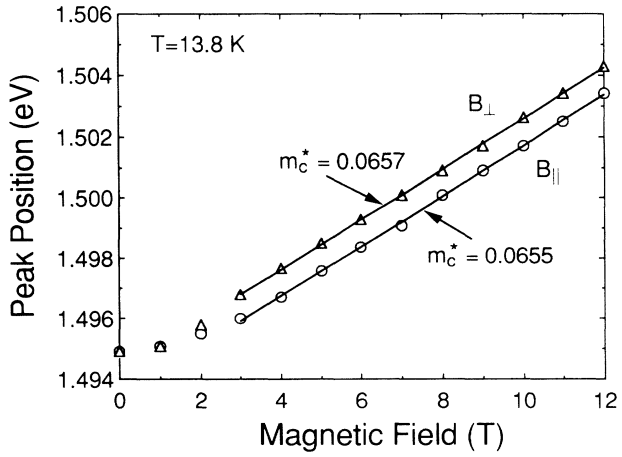

FIG. 2. As Fig. 1, for the 550-Å-period superlattice.

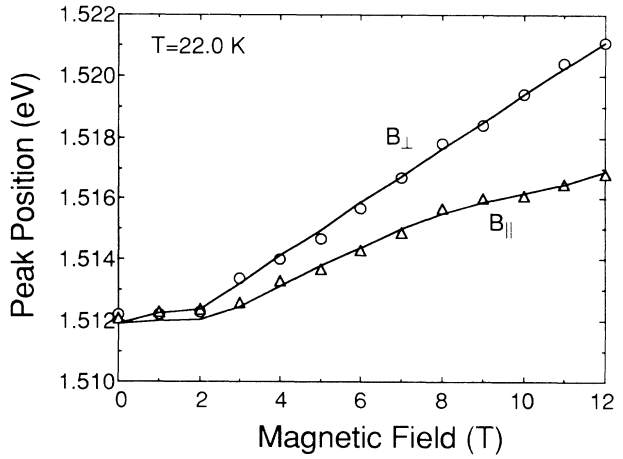

FIG. 3. As Fig. 1, but for the 153-Å-period superlattice. The solid lines are the theoretical calculation described in the text, using a cyclotron mass for perpendicular fields of $0.0653m_0$, a rigid shift of 1.9 meV to higher energy, a Gaussian FWHM=2.8 meV in the convolution of $g(E)$, and $C=3\times10^4$ in $f'(E_A)$.

matrix element; and $\delta(\cdots)$ is the energy-conserving Dirac δ function. The distribution of acceptor ions along the growth axis is not actually uniform, as assumed above; in fact, most of the acceptors are located in the AlGaAs barriers.[9] However, the present experimental data involve only the acceptors near the centers of the GaAs wells, since the shallower acceptors in or near the barriers are differentially ionized at the measurement temperature. The assumption of a uniform distribution *within* the GaAs layers should be reasonable.

We calculate $E_A(x_i)$ variationally, as will be described elsewhere. For parallel fields, $g(E)$ is computed from the Landau-level energy as a function of orbit center position, as determined from a numerical solution of Schrödinger's equation for the sum of the electrostatic and magnetic field-induced potentials.[3,4] The finite width of the barriers and appropriate matching of the wave functions at the interfaces[12] are included. For perpendicular fields, the miniband dispersion relation yields $g(E)$ directly. For both orientations, $g(E)$ includes spin splittings and is broadened by convolution with a Gaussian, to account for scattering effects.

In applying the calculation, we adjust the width of the Gaussian used to convolute $g(E)$ and the parameter C in $f'(E_A)$ to fit the line shape of the spectrum at the highest field in the perpendicular geometry. The peak positions are then fitted as a function of field, treating the cyclotron mass in this geometry and a small rigid shift of all the calculated peaks as adjustable parameters. The peak positions in the parallel geometry are then calculated using the parameters determined from the perpendicular case, with *no new fit parameters*. The results for the 153-Å-period superlattice are shown as the solid lines in Fig. 3; the agreement with experiment is seen to be excellent. We thus confirm that the nonlinear field dependence of the cyclotron energy can be accurately modeled in the miniband breakdown regime.

In conclusion, we have shown that the magnetic-field dependence of miniband-to-acceptor transitions in a GaAs/AlGaAs superlattice provides a sensitive and easily analyzed probe of cyclotron motion and related issues in miniband transport. We measured the vertical transport mass in the miniband tunneling regime, demonstrated the complete destruction of the miniband structure for magnetic lengths much shorter than the superlattice period, and obtained excellent agreement between theory and experiment in the intermediate regime involving the onset of miniband breakdown. This technique should find significant future applications, e.g., in measuring tunneling masses as a function of barrier height and width, and in exploring such issues as Γ-X mixing in short-period superlattices, etc.

This work was partially supported by the Faculty Grant-in-Aid program at Arizona State University.

[1]L. Esaki and R. Tsu, IBM J. Res. Dev. **14**, 61 (1970).

[2]J. Bleuse, G. Bastard, and P. Voisin, Phys. Rev. Lett. **60**, 220 (1988).

[3]G. Belle, J. C. Maan, and G. Weimann, Solid State Commun. **56**, 65 (1985).

[4]Jan-Kees Maan, Festkorperprobleme **27**, 137 (1987).

[5]T. Duffield, R. Bhat, M. Koza, F. DeRosa, D. M. Hwang, P. Grabbe, and S. J. Allen, Jr., Phys. Rev. Lett. **56**, 2724 (1986).

[6]T. Duffield, R. Bhat, M. Koza, F. DeRosa, K. M. Rush, and S. J. Allen, Jr., Phys. Rev. Lett. **59**, 2693 (1987).

[7]T. Duffield, R. Bhat, M. Koza, D. M. Hwang, F. DeRosa, P. Grabbe, and S. J. Allen, Jr., Solid State Commun. **65**, 1483 (1988).

[8]D. Bimberg, Phys. Rev. B **18**, 1794 (1978), and references therein.

[9]B. J. Skromme, R. Bhat, and M. A. Koza, Solid State Commun. **66**, 543 (1988).

[10]W. T. Masselink, Yia-Chung Chang, and H. Morkoç, Phys. Rev. B **32**, 5190 (1985), and references therein.

[11]S. A. Schwarz, C. L. Schwartz, J. P. Harbison, and L. T. Florez, in *SIMS VII* (Wiley, New York, 1990), p. 467.

[12]G. Bastard, Phys. Rev. B **24**, 5693 (1981).

[13]Throughout our calculations, $\Delta E_g = E_g(Al_xGa_{1-x}As) - E_g(GaAs) = 1.247x$ eV, $m_e^*(x) = 0.0665 + 0.0835x$, and $\Delta E_c/\Delta E_g = 0.69$.